www.czasopisma.pan.pl PAN POLSKA AKADEMIA NAUK www.journals.pan.pl

Arch. Metall. Mater., Vol. 61 (2016), No 3, p. 1471–1476

DOI: 10.1515/amm-2016-0241

L. KOZIELSKI*#, M. ADAMCZYK*, K. FELIKSIK*, D. BOCHENEK*, F. CLEMENS**

# PLZT MICROFIBERS TECHNOLOGY OPTIMIZATION

Electrocaloric (EC) structures for a new generation of cooling or heating elements utilize the temperature dependence of spontaneous polarization in some ferroelectric materials to convert waste heat into electricity and vice versa. A $(Pb_{0.93}La_{0.07})(Zr_{0.65}Ti_{0.35})O_3$ material, have the largest recorded pyroelectric coefficient. An effective predicted form for such applications is fiber, due to small heat capacitance and quick response time, even for nano second laser excitation. Consequently, the presented work provides a description of the optimization of structural, ferroelectric and piezoelectric properties of obtained fibers, finally concluding on necessity of sintering temperature reduction in 100°C in contrast to bulk form to effectively prevent its destruction.

*Keywords:* Electrocaloric Efect, piezoelectric fibers, ferroelectric properties

## 1. Introduction

Many of perovskite-type ferroelectrics show enhancement not only of electromechanical properties, but also abrupt change in dielectric response in the vicinity of the region so called morphotropic phase boundary (MPB). What exactly is MPB? Literally MPB means the "the boundary between two forms", however discussed materials show the compositional phase transition from rhombohedral to tetragonal phase, so the MPB is much complicated structure than simple boundary. It is more like phase region, since additional lower symmetry monoclinic phase exist between the rhombohedral and tetragonal phases. The material with the composition that belongs to MPB region demonstrates the behavior typical for relaxor ferroelectrics including the significant reduction of $\varepsilon`_{max}$ and shift of the corresponding temperature ($T_m$) towards the higher values with simultaneous frequency increase. Electrocaloric effect (ECE) is connected with the change of dipolar entropy and adiabatic temperature reversal due to application of electric field to polar materials [1,2],. The materials with the appreciable ECE can be efficient route to realize solid state cooling devices [3,4]. The application area of such devices is very wide, for example for temperature control of processors and electronic equipment as well as in on-chip cooling [5]. The advantage of most importance, is that the waste heat is directly "consumed" at the cooled device surface and transformed into useful electric energy, whereas in the traditional solution for refrigeration, the coolers are responsible only for transporting of thermal energy and its further dissipation in the air. The second attractive feature of this new solution is lack of freon emission, which usually leaks from old refrigeration systems - so that, the proposed novel idea is much more environmental friendly. The interest in alternative cooling technologies based on ECE has increased over the past decades. The materials with these features are very desirable. The attention of scientists is focused, among the other, on some organic and inorganic ferroelectric materials [6-13].

Especially attractive from presented point of view are ferroelectric relaxors (FR). FR are a group of materials, in which structural disorder play a giant role. At high temperature these materials exist in a non-polar paraelectric phase. Upon cooling they transform into state, in which polar regions of nanometer scale with randomly distributed direction of dipole moments appear [14]. It could be said that structural disorder disrupt the long-rang ferroelectric ordering and the polar – glass state is created. However the ordered state with high polarization, can be easily formed from the disordered state by electric switching. The large number of ordered polar nanoregions can give extra entropy and lead to giant ECE [14]. The discussed phenomena is more distinct in RF thin films. Neese et al. [15] and Lu et al. [4] reported, that in a thin films of PVDF and PLZT near room temperature the temperature change under an electric field of 125kV/mm was about 30K. On the other hand, among the relaxor materials the largest reported EC conversion coefficients were recorded for the $(Pb_{0.93}La_{0.07})(Zr_{0.65}Ti_{0.35})O_3$ (7/65/35 PLZT) that undergo the relaxor–ferroelectric phase transition with a maximum energy density of 1014 J/cm$^3$ per cycle [16]. In comparison, the EC energy conversion for PMN–PT near the morphotropic phase boundary (MPB) is reported at the level of only 100 mJ/cm$^3$ per cycle [17].

Taking into account the mentioned facts the authors implemented the most EC effective 7/65/35 PLZT material into innovative micro ceramics of fiber geometry to build efficient EC solid-state coolers. Such pyroelectric thin fibers allow

* INSTITUTE OF TECHNOLOGY AND MECHATRONICS, FACULTY OF COMPUTER SCIENCE AND MATERIAL SCIENCE, UNIVERSITY OF SILESIA, 12 ŻYTNIA STR., SOSNOWIEC, POLAND

** EMPA, LABORATORY FOR HIGH PERFORMANCE CERAMICS, 8600 DUEBENDORF, SWITZERLAND

# Corresponding author: lucjan.kozielski@us.edu.pl

high-power-density ultra – fast thermal energy harvesting due to extreme high surface to volume ratio.

The first encountered problem was enormous degradation of chemical composition of 7/65/35 PLZT fibers during typical for PZT type ceramics temperature synthesis at 1250°C. Consequently, the paper presents the results of research connected with the optimization of synthesis temperature and evaporation protective techniques for controlling properties of piezoelectric thin fibers considering structural, ferroelectric and piezoelectric properties.

## 2. Experimental procedure

The facts described above contributed to choosing the composition $(Pb_{0.93}La_{0.07})(Zr_{0.65}Ti_{0.35})O_3$ (PLZT 7/65/35), which is one of the closest to the MPB, for the investigation performed. The material was obtained by conventional Mixed Oxide Method (MOM) from the stoichiometric amounts of reagents which were the appropriate amount of oxides of high purity (Sigma Aldrich). To the weighted powders was added a 5% excessive amount of PbO was added in aim to compensate loses of PbO connected with its high temperature volatility.

Subsequently all the powders were milled in a planetary mill (RETCH PM400), sieved and pressed into cylindrical pellets. Next the materials were calcinated in an alumina crucible at 925°C for 3 h. The obtained samples were crushed and milled again for 24 h to finally achieve reduction in the average grain size to ~4.06 μm. In order to reach a fiber geometry the material was formed by uniaxial extrusion in Rosand Precision Ltd extruder using a steel orifice of 300 μm in diameter. The PLZT 7/65/35 fibers were then loosely placed in the special alumina rectangular crucible with a tight in the presence of protective atmosphere of $PbZrO_2$ (Fig.1). and sintered. The process of sintering was carried out for 6 h at two selected temperature $T_s$=1150°C and $T_s$=1250°C, respectively.

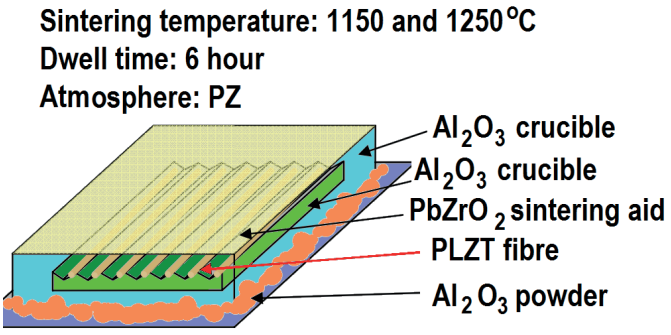


Fig.1 Special alumina rectangular crucible with a cover for creation of protective atmosphere during high temperature sintering process

The macrostructure of obtained PLZT 7/65/35 fibers sintered at two temperatures were examined in two-steps. The first one included the preliminary tests connected with the sintering shrinkage determination and was carried out using the optical microscopy technique (Leica Wild M32). The more detailed prove of the structure of fibers was conducted with using the scanning electron microscope (SEM - Vega Plus 5136MM-Tescan). In aim to examine the crystal structure the XRD measurements were carried out. The diffraction patterns were recorded using an XRD PANalytical X'Pert Pro Multipurpose Diffractometer with CuKα- radiation in a wide-angle scan from 5 to 80°, with a step width of 0.05°. For phase identification of the samples a quantitative analysis was performed by using the Rietveld refinement method based on the respective structural models. Frequency and temperature dependents of dielectric properties were measured using a computer-controlled Agilent E4980A LCR Meter in the frequency range from 100 Hz to 1 MHz. The amplitude of measuring field was equal to 1 V. The piezoelectric and ferroelectric properties of discussed materials were evaluated at room temperature using an aixPES Piezoelectric Evaluation System.

## 3. Results and discussion

### 3.1. Microstructure of PLZT 7/65/35 ceramics in fiber form

The preliminary research of obtained ceramic fibers started from the determination of shrinking process scale. The initial diameter of discussed fibers (before sintering process) was equal 300 μm. The final diameter of the fibers sintered at 1150°C and 1250°C was equal 235 μm and 243 μm respectively (Fig.2a, b and Fig.3a, b). The differences in geometric dimensions was transferred into the quality of samples obtained at higher temperature that have visibly destructed surface with a large number of pores (Fig.2c,d and Fig.3c,d). The lateral surface of lower- temperature sintered samples are more smooth.

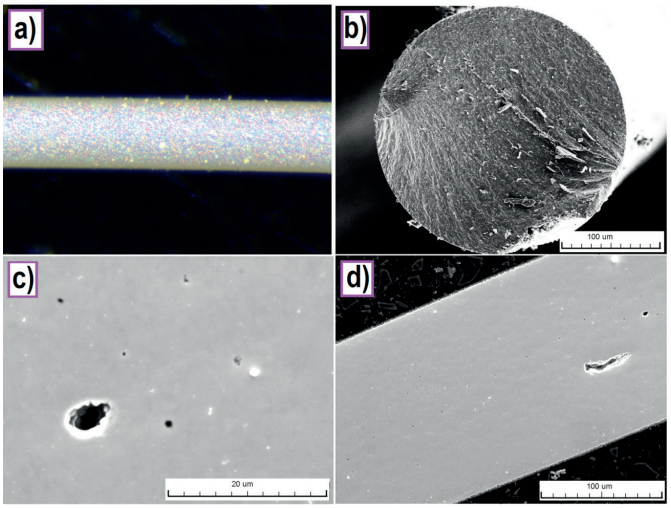


Fig. 2 Scanning electron microscope (SEM) images of PLZT ceramics in fiber form sintered at 1150 °C in 6 h; optical microscopy image of fiber surface (a) and respective SEM cross section pattern (c); polished fiber sample picture (b) and chemically etched fiber flank (d)

The careful analysis of image shown in Fig.3b reveal the presence of the secondary phase, which assumes the form of rectangular crystals. The fibers sintered at lower temperature did not reveal any secondary phase.

The Gatan Digital Micrograph software was employed to obtain the average grain size. The average diameter of grain

is dependent on the sintering temperature and equal (1.99 ± 0.53) μm and (3.06 ± 0.79) μm for fiber sintered at 1150°C and 1250°C, respectively. The bulk density, evaluated by the Archimedes displacement method, increased with decreasing $T_s$ from 7.82 to 7.70 g/cm$^3$. The changes are connected with the increasing of the mean porosity, which ranges from 1.23% ± 0.24 to 5.83% ± 4.31 for fiber sintered at 1150°C and 1250°C, respectively (Table 1).

The results presented above unambiguously show that the typical sintering temperature $T_s$=1250°C, which is usually used for bulk PZT-type ceramic materials is much higher for micro fiber technology. This effect has been discussed in more detail in the ceramic processing literature. In the case of fibers the length of diffusion paths is considerably shorter in comparison with bulk ceramics, what is resulting in significantly more effective matter transport [18]. Consequent 100°C decrease in sintering temperature is sufficient from point of view of fibers microscopic quality.

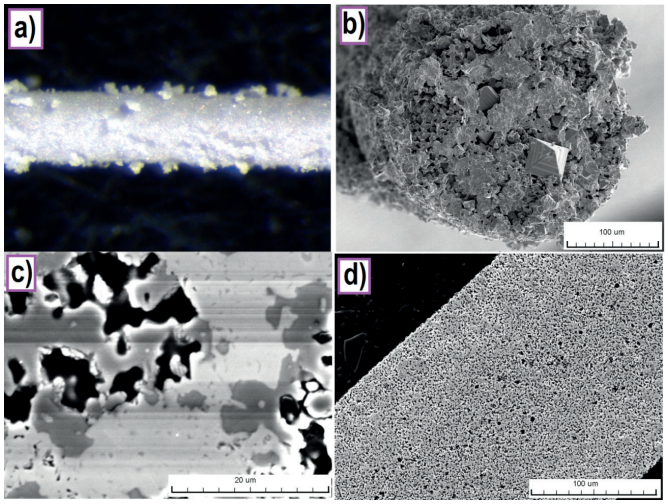


Fig.3 Scanning electron microscope (SEM) images of PLZT ceramics in fiber form sintered at 1250°C in 6 h, optical microscopy image of fiber surface (a) and respective SEM cross section pattern (c); polished fiber sample picture (b) and chemically etched fiber flank (d)

### 3.2. Structure of PLZT 7/65/35 ceramics in fiber form

It is commonly known that microstructure, crystalline and structure properties of ceramic materials is equally important, so the XRD measurements were performed. The XRD diffraction spectra of the PLZT 7/65/35 ceramics in fiber form sintered at 1150°C and 1250°C are presented in Fig.4a and 4b, respectively.

In the case of PLZT 7/65/35 fibers sintered at 1150°C the obtained results point at single phase of obtained sample and show good agreement to diffraction spectra P1 perovskite phase (ICSD collection code: 94006 [19]), with the goodness of fit parameter (GOF) of 0.9. The lattice parameters obtained from X-ray pattern for fibers sintered at 1150°C are collected in Table 1. The crystal structure of the fibers sintered at 1250°C is far from ideal, as it would be expected considering the results of microstructure investigations. First of all the samples contain a strong (43.3 %) contribution of $ZrO_2$ phase (Fig.4b), the presence of which may be affected to a significant deterioration of the ferroelectric and piezoelectric properties. The presence of secondary phase influence on the high value of GOF parameter (6.9) as well as the significant decreasing of crystal lattice unit cell volume (Table 1).

Very interesting from application point of view, as was described in introduction, is the value of anisotropic atomic displacement parameter (ADP) which compares the calculated and measured structure distortion. A high value of the parameter indicates on the tendency to disordering and creation of polar regions and consequently presence of high electrocaloric effect. Both samples, discussed in present paper, show distinctively high value of APD parameter (Table 1) corresponding to highly anisotropic [111] axial dipoles formed from off-centre Pb/La and following Ti/Zr displacements. The results are very promising results because La ions shifts are connected with the generation of random local strain fields, suppressing the long range ordering and encourage of random polar regions generation in the absence of an applied external electric field [6]. Such scenario is connected with the enhancement of electrocaloric effect.

TABLE 1

The values of sintering related coefficients for PLZT bulk samples and fibers

| PLZT ceramics parameter | | Fiber sintered at 1150 °C | Fiber sintered at 1250 °C |
|---|---|---|---|
| Shrinkage | % | 15.24 | 21.48 |
| Porosity | % | 1.23 | 5.83 |
| Grain size | mm | 1.99 | 3.06 |
| Density measured | g/cm$^3$ | 7.82 | 7.70 |
| Density calculated (XRD) | g/cm$^3$ | 7.9450 | 8.5842 |
| Lattice parameter a | Å | 5.7783(4) | 5.6113(6) |
| Lattice parameter b | Å | 5.7959(3) | 5.6368(6) |
| Lattice parameter c | Å | 5.7668(4) | 5.5947(6) |
| Unit cell volume V | Å$^3$ | 136.4505 | 126.2894 |
| Anisotropic displacement parameter | [-] | 3.78 | 4.5 |

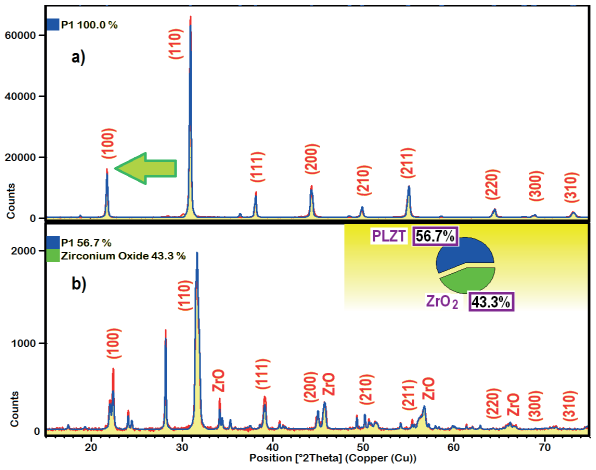


Fig.4 XRD profiles for the PLZT 7/65/35 fibers sintered at 1150°C (a) and 1250°C (b); indicator of textured P1 phase has been indicated by arrow

### 3.3. Dielectric and piezoelectric measurement of PLZT 7/65/35 ceramics in fiber form

The temperature dependences of dielectric permittivity and loss factor for the PLZT 7/65/35 fibers sintered at 1150°C and 1250°C are presented in Fig.5a and b, respectively. Significantly higher values of dielectric constant are visible for the PLZT 7/65/35 samples sintered at 1150°C as well as distinct maximum presence indicating phase transition (Curie Temperature $T_C$), whereas in case of fibers sintered at 1250°C there were no visible maxima in this characteristics (Fig.5b). An adequate trend is observed in the dielectric loss tangent (tanδ) temperature dependency in both pictures, and the dielectric loss for PLZT 7/65/35 sintered at 1150°C are one order of magnitude lower than for the PLZT 7/65/35 fibers sintered at 1250°C.

As it was expected, based on structural, microstructural and dielectric properties the PLZT 7/65/35 fibers sintered at 1150°C become highly stress sensitive resulting in excellent

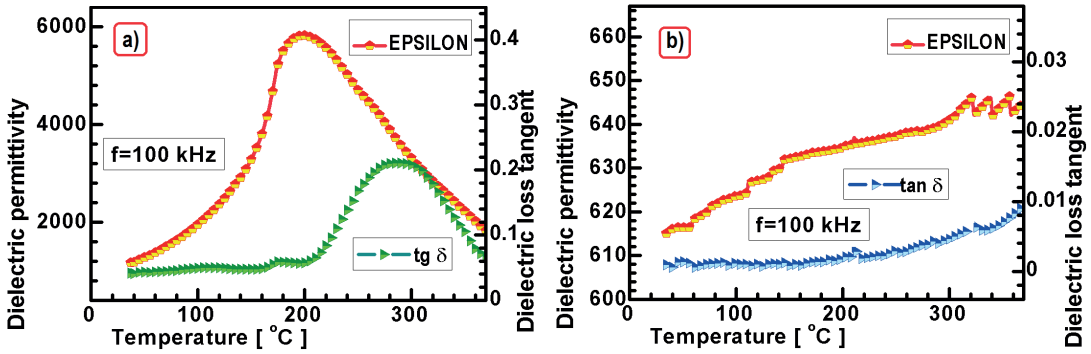


Fig.5 A variation of dielectric constant and dielectric loss tangent with temperature for the sintered at 1150°C (a) and 1250°C (b) PLZT 7/65/35 fiber measured at a frequency of 100 kHz

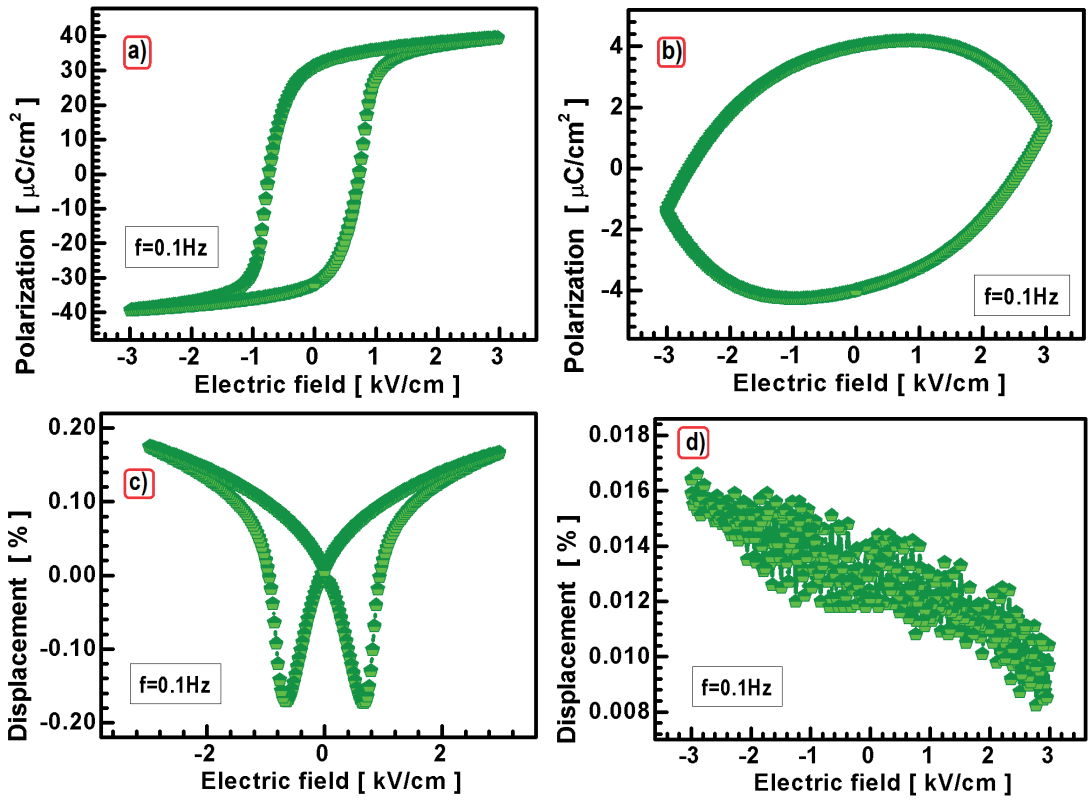


Fig.6 A variation of ferroelectric hysteresis (a and c) and strain evolution (SE) loop (b and d) for the sintered at temperature of 1150°C and 1250°C fiber PLZT samples, respectively

ferroelectric and piezoelectric properties as shown in Fig.6a and c, in contrast to hardly observed effects in samples obtained in the temperature of 1250°C (Fig.6b and d). It should be noted that for fibers sintered at 1150°C the value of displacement induced by electric field is equal 0.35 %. The obtained value stay in consistency with literature data for discussed composition in form bulk [20], in spite of short radius and strong surface effect, which is present in micro fibres form of ceramics. This fact is probably also connected with significant texture indicator along [100] crystallographic direction (the intensity of line (100) marked by green arrow in Fig.4a). It seems, that the texture, which was revealed in XRD measurements, is connected with the technology of fibres. Namely application of the uniaxial extrusion method leads to ordering grains of powder of PLZT 7/65/35 according their shape connected with certain preferred crystallographic distribution. In consequence in spite of microstructural deficiency obtained material is characterized by very high piezoelectric coefficient $d_{33}$= 322 pC/N.

## 4. Conclusions

The presented work developed and implemented technology for controlling properties of piezoelectric thin fibers for electrocaloric applications providing comparative analysis between fibers of the same PLZT 7/65/35 material but sintered at 1250°C and 1150°C for 6 h. Subsequently, set of characteristics were shown in order to explain the huge differences found in structural, ferroelectric and strain properties. Finally the experiment proved that decrease of 100°C in sintering temperature enables to obtain high performance piezoelectric fibers.

### Acknowledgements

This research was supported by the National Centre for Research and Development, grant no. TANGO1/267100/NCBR/2015.

## REFERENCES

[1] M. Lines, A. Glass, Principles and Applications of Ferroelectrics and Related Materials, Oxford 1977.
[2] E. Fatuzzo, W.J. Merz, Ferroelectricity, Amsterdam 1967.
[3] T. Mitsui, I. Tatsuzaki, E. Nakamura, Introduction to the Physics of Ferroelectricity, London 1976.
[4] G. Lu, B. Rozic, Q.M. Zhang, Z. Kutnjak, R. Pirc, M. Lin, X. Li, L. Gorny, Appl. Phys. Lett. **97**, 202901, 1-3 (2010).
[5] B. Rozic, M. Kosec, H. Ursic, J. Hole, B. Malic, Q.M. Zhang, R. Blinc, R. Pirc, Z. Kutnjak, J. Appl. Phys. **110**, 064118, 1-5 (2011).
[6] A.S. Mischenko, Q. Zhang, J.F. Scott, R.W. Whalmore, N.D. Mathur, Science **311**, 1270-1276 (2006).
[7] B. Neese, B. Chu, S.G. Lu, Y. Wang, E. Furman, Q.M. Zhang, Science **321**, 821-824 (2008).
[8] F. Scott, Science **315**, 954-959 (2007).
[9] A.S. Mischenko, Q. Zhang, R.W. Whatmore, J.F. Scott, N.D. Mathur, Appl. Phys. Lett. **89**, 242912 1-3 (2006).
[10] G. Akcay, S.P. Alpay, G.A. Rossetti, J.F. Scott, J. Appl. Phys. **103**, 024104, 1-7 (2008).
[11] D. Guyomar, G. Scbald, B. Guiffard, L. Scvcyrat, J. Phys. D: Appl. Phys. **39**, 4491 (2006).
[12] S. Prosandeev, I. Ponomareva, L. Bcllaichc, Phys. Rev. B **78**, 052103, 1-4 (2008).
[13] S. Kar-Narayan, N. D. Mathur, J. Phys. D: Appl. Phys. **43**, 032002 (2010).
[14] A.A. Bokov, Z.G. Ye, J. Mater. Sci. **41**, 1, 31-52 (2006).
[15] B. Neese, S.G. Lu, Baojin Chu, Q.M. Zhang, Appl. Phys. Lett. **94**, 042910, 1-7 (2009).
[16] F.Y Lee, H. Jo, C. Lynch, L. Pilon, Smart Mater Struct. **22**, 025038-025054 (2013).
[17] R. Kandilian, A. Navid, L. Pilon, Smart Mater Struct. **20**, 055020-055030 (2011).
[18] M.N. Rahaman: Ceramic Processing, Kirk-Othmer Encyclopedia of Chemical Technology 2014
[19] H. Liu, R. Harrison, A. Putnis, J. Appl. Phys. **90**, 6321-6326 (2001).
[20] G.H. Haertling, J. Am. Ceram. Soc. **82**, 797-818 (1999).